Cancer Letters 618 (2025) 217638

Contents lists available at ScienceDirect

Cancer Letters

journal homepage: www.elsevier.com/locate/canlet

Original Articles

Pre-treatment DNA methylome and transcriptome profiles correlate with melanoma response to anti-PD1 immunotherapy

Sultana Mehbuba Hossain [a,b], Gregory Gimenez [a,b], Peter Stockwell [a,b], Robert Weeks [a,b], Suzan Almomani [a,b], Gregory T. Jones [c], Magdalena Ratajska [a,b,d], Mathew Shuen [a], Basharat Bhat [c], Janusz Ryś [e], Bozena Cybulska-Stopa [f,g], Agnieszka Harazin-Lechowska [e], Euan Rodger [a,b], Christopher Jackson [h], Aniruddha Chatterjee [a,b,1], Michael R. Eccles [a,b,*,1]

[a] Department of Pathology, Dunedin School of Medicine, University of Otago, Dunedin, New Zealand
[b] Maurice Wilkins Centre for Molecular Biodiscovery, Level 2, 3A Symonds Street, Auckland, New Zealand
[c] Department of Surgical Sciences, University of Otago, Dunedin, New Zealand
[d] Department of Pathology and Neuropathology, Medical University of Gdansk, Gdansk, Poland
[e] Department of Tumor Pathology, Maria Sklodowska-Curie National Research Institute of Oncology, Krakow Branch, Krakow, Poland
[f] Department of Clinical Oncology, Lower Silesian Oncology Center, Pulmonology and Hematology, Wroclaw, Poland
[g] Department of Hematology and Oncology, Faculty of Medicine, Wroclaw University of Science and Technology, Poland
[h] Department of Medicine, Dunedin School of Medicine, University of Otago, Dunedin, New Zealand

ARTICLE INFO

Keywords:
Melanoma
Immunotherapy
DNA methylation
Gene expression
Immune checkpoint inhibitors

ABSTRACT

Successful immune checkpoint inhibitor (ICI) therapy occurs in only a fraction of melanoma patients, and yet all patients are susceptible to potentially serious ICI-related side-effects. No current biomarkers robustly predict ICI treatment response in melanoma patients. In this study we sought to identify methylome and transcriptome markers which have the potential to predict immunotherapy response in melanoma patients ahead of treatment with anti-PD1 ICI monotherapy. Using Infinium MethylationEPIC microarrays, we analysed DNA methylation profiles of >850,000 CpG sites in pre-treatment melanoma tissues from patients administered anti-PD-1 monotherapy as first-line treatment. In addition, we analysed transcriptomes using RNA-seq. DNA methylation and gene expression data were then statistically compared to patient response to anti-PD1 therapy. We identified 2579 DNA hypomethylation and hypermethylation alterations correlating with melanoma response to anti-PD1 therapy. An integrative analysis of DNA methylomes and transcriptomes identified a subset of 35 loci, 13 of which were significantly differentially methylated in both initial discovery and external validation datasets. Functional enrichment analysis of hypomethylated sites (p-value <0.05) in non-responders was associated with "Formation of the cornified envelope", "Regulation of epithelial cell proliferation", and "Purine-containing compound metabolic process". We have identified novel integrated DNA methylation and gene expression markers, which correlate with anti-PD1 treatment response in melanoma patients. These findings suggest a relationship between tumour-associated genomic DNA methylation, gene expression patterns, and anti-PD1 ICI immunotherapy response in melanoma patients.

1. Introduction

Immune checkpoint inhibitor (ICI) therapies have led to improved clinical response and long-term survival benefits for patients with advanced melanoma [1]. ICI therapy of melanoma employs monoclonal antibodies to bind to immune checkpoint proteins, such as cytotoxic T lymphocyte-associated antigen 4 (CTLA-4), programmed cell death protein 1 (PD-1), or its ligand (PD-L1) to alleviate tumour-induced immunosuppression of T cells, thereby enhancing antitumour effects [2,3]. However, the success of ICI critically depends on the stepwise progression of the immunologic events within the tumour microenvironment (TME): the phenotype of the melanoma tissue (proliferative

* Corresponding author. Department of Pathology, Dunedin School of Medicine, University of Otago, Dunedin, New Zealand.
E-mail address: michael.eccles@otago.ac.nz (M.R. Eccles).
[1] These authors contributed equally as joint senior authors.

https://doi.org/10.1016/j.canlet.2025.217638
Received 29 November 2024; Received in revised form 20 February 2025; Accepted 11 March 2025
Available online 13 March 2025

state versus dedifferentiated state), the abundance of expressed neoantigens, and the presence of activated immune cell populations, including macrophages, which contribute largely to ICI therapy response in melanoma [4,5]. A recent study has reported that ICI therapy targeting only immune cells (CTLA-4 and PD-1), has a more effective anti-tumour response compared to ICI therapy that targets tumour cells (PD-L1) [6], which may result from activation of the immune system against neoantigens. Activation of the immune system can lead to secondary toxicities arising from altered immune cell function and cytokine release from immune and non-immune cells in the TME [6]. However, not all patients respond to ICI therapy, and some patients respond better to one type of ICI therapy than to others [7,8] and so there remains a need for predictive biomarkers that facilitate patient selection and treatment decisions.

Detection of PD-L1 using immunohistochemistry is a widely used biomarker for predicting ICI therapy response in melanoma and other cancer types [9]. However, PD-L1 protein expression as a single biomarker has marked limitations in predicting response to ICI anti-PD1/PD-L1 therapy [10]. Recent evidence strongly suggests that patients with high PD-L1 expression, together with absence of tumour infiltrating lymphocytes (TILs) (i.e. "constitutive PD-L1") show worse response rates than patients with PD-L1 expression and the presence of TILs (i.e. "inducible PD-L1") [11,12]. We previously [13] showed that DNA methylation patterns distinguish between inducible versus constitutive PD-L1 expressing cell lines, which were derived from melanoma patients (referred to therein as PD-L1-inducible and PD-L1 constitutive, or $PD\text{-}L1_{IND}$ and $PD\text{-}L1_{CON}$). Global hypomethylation was associated with upregulation of PD-L1 expression in $PD\text{-}L1_{CON}$ melanoma cell lines. Several clinical trials have also shown that the combination of epigenetic therapy (such as decitabine, which is an inhibitor of DNA methylation) with ICI immunotherapy may lead to markedly improved patient responses [14,15]. Taken together, the evidence suggests that global DNA methylation levels have an important role in controlling PD-L1 expression in cancer cells, and that certain epigenetic configurations underpin immunotherapy resistance in melanoma. Therefore, in this study we hypothesized that responder and non-responder melanomas to ICI therapy would contain epigenetic constitutions that are distinct from one another.

Here we have investigated genome-wide DNA methylation differences in relation to ICI response in melanoma patients, and we have additionally integrated these DNA methylation findings with changes in mRNA expression levels, to better understand the functional role of the identified DNA methylation and transcriptional differences in relation to treatment outcomes. Successful identification of specific DNA methylation biomarkers for melanoma may lead to better understanding of epigenetic contributions to regulation of the immune system in melanoma patients, potentially with impacts to allow stratification of patients for ICI treatment, and ultimately improving melanoma patient outcomes and survival. Furthermore, identification of DNA methylation differences could potentially represent a more stable and more sensitive class of ICI response biomarkers than, for example, differences in gene or protein expression levels for the prediction of ICI treatment response.

2. Methods

2.1. Clinical characteristics of melanoma patients and collection of melanoma samples

Ethical approval for the experimental work was granted by the Maria Sklodowska-Curie National Research Institute of Oncology Ethics Committee, Krakow, Poland (KB/430-74/20), and all patients provided informed consent (KB/430-74/20). We retrospectively identified melanoma patients in collaboration with the Maria Sklodowska-Curie National Research Institute of Oncology, Krakow, Poland. This study employed the following inclusion criteria: (i) age $\geq$18 years, (ii) Underlying histologically confirmed melanoma, (iii) who had received/are receiving Pembrolizumab or Nivolumab treatment (monotherapy, anti-PD1) for advanced stage IV cutaneous melanoma, (iv) who did not receive any previous cancer treatment prior to tissue biopsy, (v) where sufficient tissue was retrieved from primary metastatic lymph node dissections (where available) or primary tumour tissue, and (vi) formalin-fixed paraffin-embedded (FFPE) tumour tissue prior to the start of anti-PD-1 ICI therapy was available. Clinical data collected from melanoma patients included the baseline characteristics of patients, survival time and cause of death (Supplementary Table 1). Radiological assessment of response was defined according to the Response Evaluation Criteria in Solid Tumours for immune-based therapeutics (iRECIST criteria) and performed by independent radiologists from the centres.

2.2. Genome-wide DNA methylation analysis

Melanoma specimens that were sampled before the first administration of anti-PD-1 ICI therapy, which contained $\geq$60 % of tumour cells, as evaluated by pathologists, were selected for the analysis. Macrodissected FFPE tissue samples were used to extract DNA using an QIAamp DNA FFPE Tissue Kit, followed by DNA quantification (Qubit™ HS DNA reagent) and quality assessment (Illumina FFPE QC Kit).

Subsequently, 500 ng of extracted DNA from each FFPE sample was used for bisulfite conversion using EZ DNA Methylation-Gold Kit (Zymo Research, Irvine – USA). All samples were bisulfite converted and analysed using Infinium MethylationEPIC v1.0 BeadChips (Illumina), following the manufacturer's protocol. In total, 17/40 melanoma tumour DNA samples successfully passed the Illumina FFPE QC quality control assay, as well as an additional quality control assay performed following bisulfite conversion.

2.3. Data analysis for infinium MethylationEpic Beadchips assay

The RnBeads package was used to load raw microarray data (.idat files) into the statistics program RStudio (Version February 1, 5042, R Foundation for Statistical Computing, Vienna, Austria) for initial quality control, pre-processing and differential methylation analysis [16], as previously described [17]. Data normalization was performed using *missMethyl*, *watermelon*, *methylumi* (*bmiq*) packages. A false discovery rate of 5 % on the analysed sites (at an alpha level = 0.05) was applied to filter for significant probes.

2.4. RNA sequencing and data analysis

RNA was extracted from macrodissected FFPE tissue samples using Qubit™ HS (high sensitivity) RNA reagent and RNA-Sequencing was performed with single-end reads, read length of 101 basepairs and 20 million reads to produce raw fastq files as previously described [4]. The data are available in GEO: GSE213145. RNA-Seq data analysis was performed as described previously [18]. Briefly, RNA-Seq reads were trimmed for adaptor sequences using the cutadapt tool and clean reads were then mapped to the GRCh37 assembly with the gene, transcript, and exon features of Ensembl using HISAT2 [19]. Read counts for each sample were retrieved, first by exon, and then summarized by gene using featureCounts [20]. For filtering, genes with 5 or lower counts in at least five samples were removed before differential expression analysis. Genes with low counts make up a significant proportion in RNA-seq datasets and can reduce power in the differential expression analysis [21]. Differential expression analysis was performed using the DESeq2 method [22]. An FDR adjusted p-value threshold of 0.05 was used to call significant genes. The normalized gene expression levels were measured in TPM (Transcripts Per Million) values.

2.5. Targeted bisulfite methylation library preparation

Primers used for analysing four genomic loci were designed using the MethPrimer program [23]. The sequences of the primers are given in

Supplementary Table 2. Illumina oligo sequences for forward primer "ACGACGCTCTTCCGATCT" and for reverse primer "CGTGTGCTCTTCCGATCT". Targeted bisulfite sequencing was then performed using reagents and primers as described in Supplementary Tables 3–5.

2.6. Computational analysis of targeted methylation sequencing data

The sequenced reads were assessed using in-house developed bioinformatics tools. Read quality of sequences was checked using FastQC, followed by joining the R1 and R2 accurate pair-end read merger for all the samples using PEAR [24]. The adapters were removed from the sequences and also the low-quality reads (Phred score of 20) were removed using Trim_Galore (https://github.com/FelixKrueger/TrimGalore), followed by splitting multiple fastq files by matching barcodes using Barcode Splitter. Alignment of the reads with target genomic regions and generating methylation scores were performed using BIQ Analyzer [25]. All graphs for targeted methylation libraries were prepared using GraphPad Prism version 9.

2.7. Tumour mutation burden panel analysis

DNA quantification for Ion AmpliSeq™ Library Preparation was performed using TaqMan® RNase P Detection Reagents, following the manufacturer's instruction (ThermoFisher). DNA samples were analysed using Oncomine™ Tumor Mutation Load Assay (ThermoFisher, Melbourne, Australia). The resulting data were received in BAM file format for further analysis. Initial analysis was conducted using the Oncomine Tumour Mutation Load – w3.0 – DNA – Single Sample workflow on the Ion Reporter cloud server. All samples passed in-built QC (quality control) test, achieving ≥80 % uniformity in depth of reads across the whole genome. Mutation loads were then calculated as mutations per megabase (Mutations/MB) for each sample, with statistical significance at p-value <0.05. We used Ion Reporter™ Software algorithm to calculate tumour mutational burden (TMB) using following formula:

$$TMB = \frac{(SM \times 10^6)}{Total\ exonic\ bases\ with\ sufficient\ coverage}$$

- TMB = Tumour mutational burden
- SM = Somatic mutations

2.8. Bioinformatic analysis of online available data

Publicly available Illumina MethylationEPIC Beadchip melanoma data from patients who received anti-PD1 (nivolumab, pembrolizumab) monotherapy, cytotoxic T-lymphocyte associated protein 4 inhibitor (anti-CTLA4, ipilimumab) monotherapy, or combination therapy of anti-PD1 (nivolumab) and anti-CTLA4 (ipilimumab), were accessed from NCBI (GEO: GSE235122) [26]). Raw.idat files were downloaded and processed using the RnBeads package, applying similar techniques and packages as described above.

3. Results

3.1. Clinical characteristics of melanoma patients and melanoma tumour samples

Melanomas from patients who received only anti-PD1 monotherapy as first-line therapy were investigated in this study for transcriptomic or methylomic markers that correlated with melanoma response to immunotherapy [27–30]. From an initial 87 melanoma patients, 40 patients were retrospectively selected for this study who had received anti-PD-1 monotherapy (nivolumab or pembrolizumab), and from whom melanoma tissue samples for analysis of DNA methylation and transcriptomic signatures were available prior to treatment starting [4]. All patients receiving combination immunotherapy, or either targeted therapy or chemotherapy before receiving anti-PD1 therapy were excluded, or patients who had initiated their anti-PD1 therapy before tissue biopsy was performed, including patients whose biopsy samples were from a distant metastasis and were taken after treatment started, were excluded (Fig. 1).

Melanoma samples were included where sufficient melanoma tumour tissue was resected from either the primary melanoma site, or from lymph node metastases in excess to diagnostic requirements, prior to the start of ICI treatment. iRECIST criteria were used to define patients as responders [31], as follows – complete response (CR), partial response (PR), or stable disease (SD) of greater than 6 months with no progression. Non-responders were defined as progressive disease (PD) or SD for less than or equal to 6 months before disease progression. Patients who received at least one cycle of anti-PD-1 ICI were evaluated for treatment response. Patients who received one cycle of anti-PD-1 ICI and who died before the first restaging during ongoing ICI therapy in the case of early progression were identified as non-responders (Supplementary Table 1). Patients in this study were stratified into 20 responders and 20 non-responders (Fig. 1). The pathology reviews of the melanoma samples are described in Supplementary Table 1 [4].

3.2. Profiling of melanoma DNA methylation patterns in melanoma tissues prior to anti-PD1 ICI treatment; correlation between methylation and response to anti-PD1 ICI therapy

We used Illumina MethylationEPIC microarray profiling to assess differences in tumour DNA methylation profiles of melanoma patients between patients who responded (n = 7) versus patients who did not respond to anti-PD1 therapy (n = 10), which were analysed using the RnBeads package [16]. In total 651,887 Illumina MethylationEPIC microarray probes sites passed QC assessment for all FFPE samples. These probes were then utilized for further statistical evaluation (Supplementary Fig. 1A). Following filtering and normalization (Supplementary Fig. 1B), 40,304 CpG probes were distributed between gene promoters (24,279 in CpG islands), and gene bodies (31,053 CpGs) [32]. The methylation differences between responding and non-responding patients to anti-PD-1 ICI treatment are summarized in a volcano plot, where yellow dots signified 270 CpGs displaying ≥30 % methylation difference and a p-value of <0.05 between responding and non-responding melanomas (Supplementary Fig. 1C).

We next investigated methylation differences between responding and non-responding patients to anti-PD1 therapy using RnBeads. This analysis resulted in 2579 significantly differentially methylated CpG sites (DMPs, p-value <0.05) with ≥20 % methylation difference between responding and non-responding melanomas (Fig. 2A). These DMPs can be divided into 1573 hypomethylated DMPs and 1006 hypermethylated DMPs in responders compared with non-responders. Mapping of these DMPs to their genomic position in the context of gene-associated regions, revealed that 50.22 % of hypomethylated DMPs were found in gene bodies, 28.73 % were found in transcriptional start sites (TSS), and 13.99 % in 5' untranslated regions (UTRs) (Fig. 2B).

3.3. Mutational load is not associated with melanoma methylation patterns nor response status

Generally cutaneous melanomas in the European population arise from epithelium-associated melanocytes in cutaneous sites with varying degrees of cumulative sun damage (CSD), as characterized by WHO in 2018 [33]. CSD is correlated with tumour mutation burden (TMB) [33]. Accordingly we categorized TMB into tiers: low (≤5 Mutations/MB), medium (≥6 and < 20), high (≥20 and < 50) and very high (≥50), based on thresholds established in the literature [34]. Our analysis revealed that 6/10 melanomas from non-responder patients to anti-PD1 therapy exhibited medium to high mutational load, while conversely, 3/7

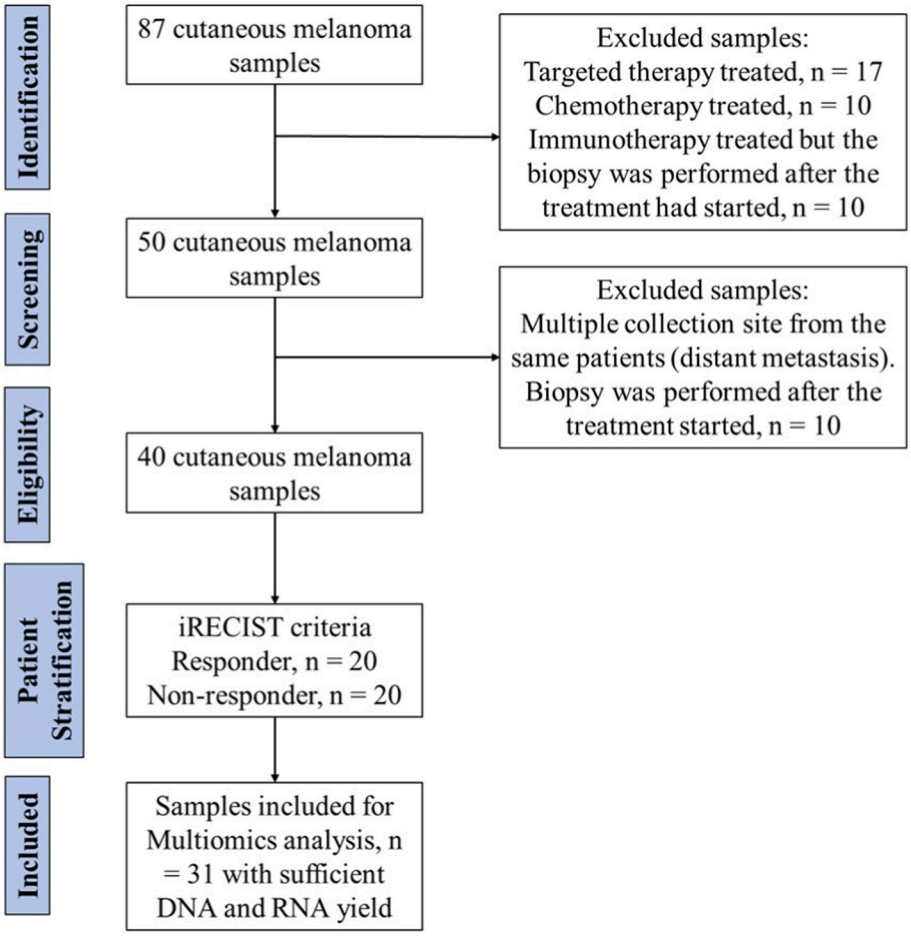

Fig. 1. Characterization and selection of patients for this study.

responder melanomas showed medium to very high mutational load (Fig. 1A). No significant correlation was observed between TMB and methylation-specific patterns. Previously, we had reported that neither mutational load, nor specific gene mutations were associated with response status or gene expression changes in melanomas from responders versus non-responders to anti-PD1 therapy [4].

3.4. Functional characterization of differentially methylated genes in melanomas prior to anti-PD1 ICI treatment

To determine the biological significance of methylation sites identified with ≥20 % methylation difference, we conducted a pathway enrichment analysis using Metascape [35]. Specifically, pathway enrichment analysis focused on differentially methylated genes in the transcription start site (TSS) region between responders and non-responders to anti-PD1 therapy.

Responding melanomas predominantly exhibited hypomethylated TSS sites associated with biological processes such as "Epithelial cell differentiation" (e.g. *DLG1*, *DLX5*, *FLT1*, *HLX*, *ZEB1*, *TGFB2*), "Stem cell differentiation" (e.g. *RUNX2*, *CD34*, *HMX2*, *SOX9*, *WNT5A*, *WNT10B*), "Regulation of fibroblast growth factor receptor signalling pathway" (e.g. *OTX2*, *PRKD2*, *SMOC2*, *FGF9*), and "Regulation of neuron differentiation" (e.g. *ATOH1*, *BDNF*, *FOXG1*, *HOXD3*, *SOX8*) (Fig. 3A). In contrast, non-responding melanomas showed enrichment of hypomethylated TSS sites related to processes like "Formation of the cornified envelope" (e.g. *JAG2*, *DCT*, *GRHL3*, *GJB3*, *BMPR2*), "Regulation of epithelial cell proliferation" (e.g. *HMGB1*, *ZNF304*, *SFRP2*, *GDF2*, *HOXA4*, *JAG2*), "Purine containing compound metabolic process" (e.g. *PRKAG3*, *ATPA12*, *GMPR*, *ACSM5*, *ACSL1*), "Cell-cell junction assembly" (e,g. *CDH13*, *CLDN5*, *NR1H4*, *PKP3*), and "Blood vessel remodelling" (e.g. *AXL*, *BMPR2*, *NPR3*, *AOC1*, *SFRP2*) (Fig. 3B). Additionally, a statistically significant over-representation of CpG sites were found to be associated with developmental processes, and the transport of proteins into the mitochondrial membrane.

3.5. Transcriptomic characterisation of melanomas prior to anti-PD1 ICI treatment

RNA sequencing (RNA-seq) was performed [4] to assess transcriptomic differences between responder (n = 10) and non-responder melanoma patients (n = 10) to anti-PD1 therapy (GEO: GSE213145). The RNA-seq analysis revealed 315 significantly differentially expressed genes (DEGs, adjusted p-value ≤0.05) between the two groups of melanomas (Fig. 4A). Among these DEGs, 170 genes exhibited ≥1.5-log2-fold difference in expression level between responders and non-responders (adjusted p-value ≤0.05) (Fig. 4B). We used 1.5-log2-fold cut-off criteria in DEGs which includes 64 protein-coding RNAs, 38 long non-coding RNAs (lncRNAs), 5 microRNAs (miRNAs or pre-miRNAs), 10 small nucleolar RNAs, 5 T-cell receptor alpha joining mRNAs and other pseudogenes.

3.6. Expression patterns of key immune-related genes between responder and non-responder melanomas

For the non-responder melanoma group, differentially expressed protein coding genes included mesenchymal transition genes, such as *OR7D2* (4.33-log2fold), *TYRP1* (3.9-log2fold), *TCN1* (3.65-log2fold), *KIT* (3.05-log2fold), *S100A2* (2.89-log2fold), *GPRC5A* (2.08-log2fold)

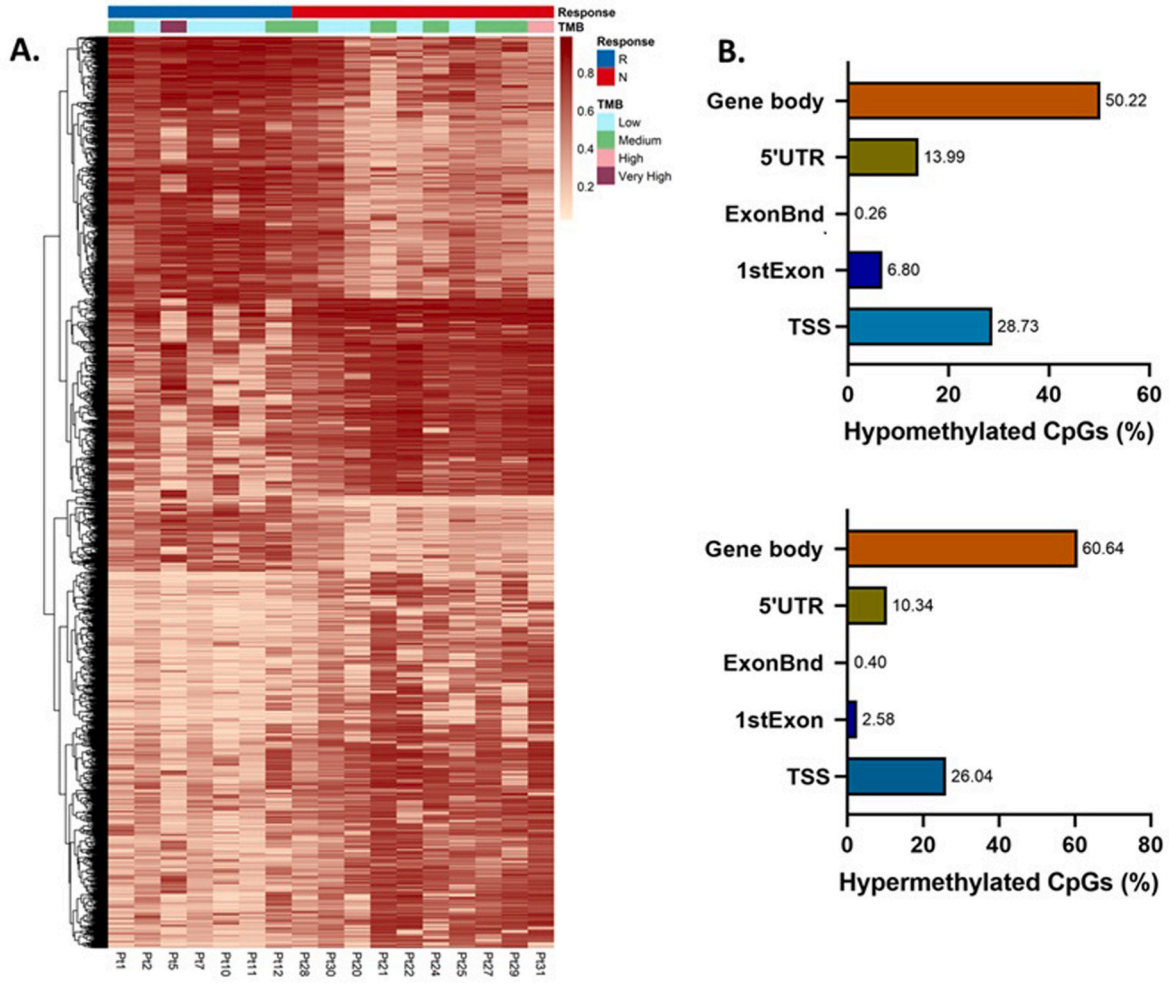

Fig. 2. Differential methylation analysis between responding and non-responding melanomas. A. Heatmap showing the differentially methylated CpG sites (DMPs). Response - blue and red representing responder and non-responder melanoma groups, respectively; Tumour mutation burden (TMB) – low, medium, high and very high; beta values are depicted on the heatmap with a range from 0 (ivory) to 1 (red) as shown. B. Percentage of DMPs located in certain genomic context between responding and non-responding melanomas.

and *NDUFA4L2* (1.58-log2fold) (Fig. 4C). In contrast, the responder melanoma group showed more than 2-log2fold upregulation of T-cell receptor alpha joining genes (*TRAJ26*, *TRAJ23*, *TRAJ19*, *TRAJ12*, *TRAJ22*) (Fig. 4C).

The expression levels of multiple well-known immune checkpoint mRNAs were further analysed between responder and non-responder melanomas. None of the immune checkpoint mRNAs were significantly differentially expressed between the responding and non-responding melanomas (Supplementary Fig. 2).

3.7. Coordinated methylome and transcriptome alterations between responder and non-responder melanomas

Using DNA and RNA isolated from the same samples, an integrated methylome and transcriptome analysis was conducted to examine differentially methylated CpGs located within gene bodies or regulatory regions (e.g. promoters/enhancers), together with significant differential expression levels of the associated genes. This approach aimed to identify methylation changes with potentially linked transcriptomic alterations, which might contribute to the coordinated response to anti-PD1 therapy in melanoma.

In total, we identified 43 differentially methylated CpGs, which were linked to the corresponding protein-coding genes with significant differential expression (Fig. 5A). The results suggested that for these genes there was a correlation between methylation and gene expression changes. Notably, 35 of these 43 CpGs demonstrated significant correlation both at the level of differential methylation and gene expression, as evidenced by Pearson correlation coefficients >0.5 and p-values <0.05 (Supplementary Table 6). For example, *COL9A2* and *ADRB1* exhibited negative correlations between transcription start site (TSS) methylation and gene expression (Pearson correlation $= -0.84$, p-value $= 0.001$; Pearson correlation $= -0.72$, $p = 0.01$, respectively). Similarly, *PRKAA2* and *TSPEAR-AS1* showed positive correlations between methylation in the gene body and increased expression (Pearson correlation $= 0.84$, $p = 0.001$; Pearson correlation $= 0.75$, $p = 0.01$, respectively). Gene promoter TSS methylation was generally associated with gene silencing, while gene body methylation showed a context-dependent influence on expression, with some genes exhibiting positive correlations. For instance, *CHADL* methylation (TSS1500; Pearson correlation $= -0.80$, $p = 0.01$) was negatively correlated with expression, whereas *F11-AS1* methylation (gene body; Pearson correlation $= 0.80$, $p = 0.001$) was positively correlated.

These findings were then followed up with a functional enrichment analysis, which revealed that these differentially methylated/expressed genomic loci were associated with pathways related to “Synaptic signalling”, “Hippo signalling regulation”, “Regulation of membrane potential”, and “Intracellular chemical homeostasis” (Fig. 5B). This analysis highlights potential molecular mechanisms underlying the

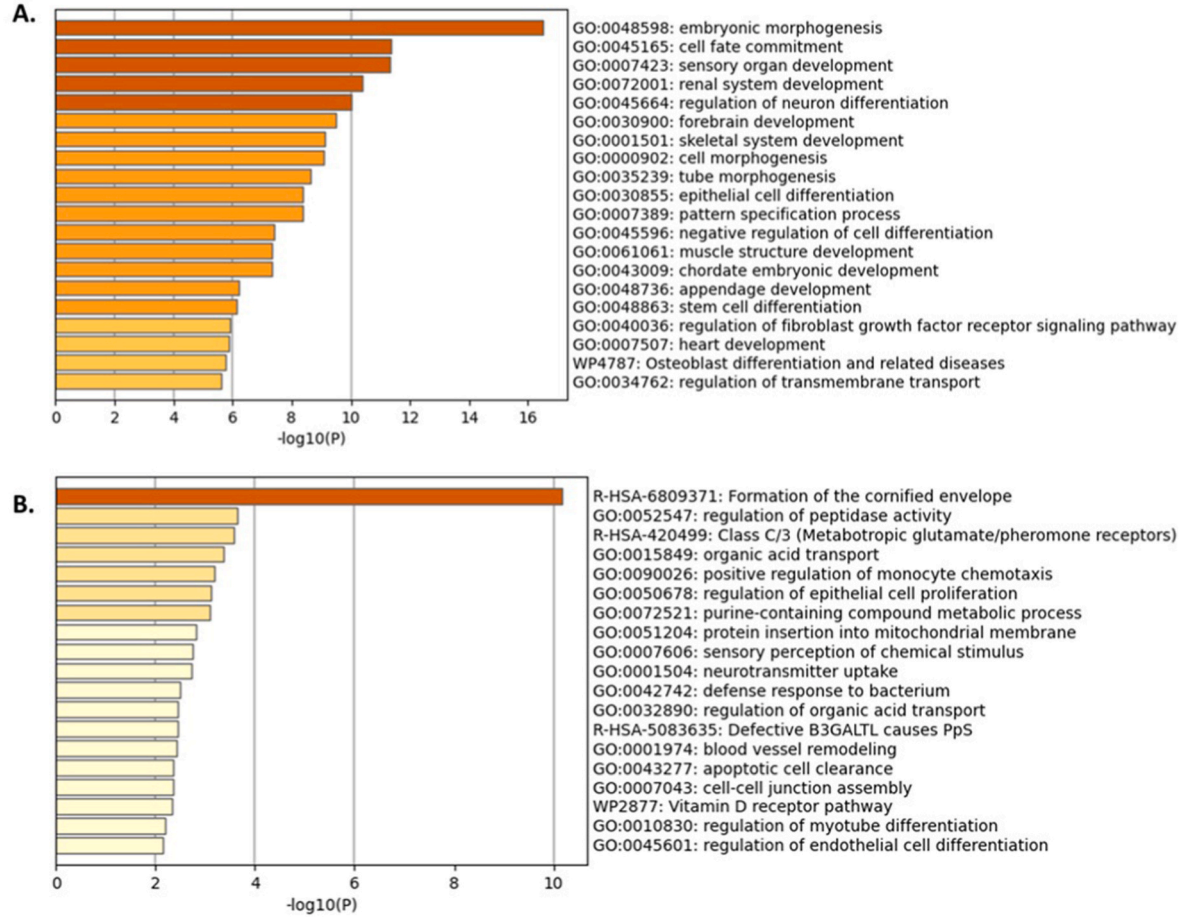

Fig. 3. Pathway enrichment analysis for differentially methylated transcription start sites (TSS) region between responders and non-responders to anti-PD1 therapy. A. Pathways enriched with hypomethylated genes in responding melanomas. B. Pathways enriched with hypomethylated genes in non-responding melanomas.

response to anti-PD1 therapy in melanoma, linking specific methylation changes with corresponding alterations in gene expression and pointing towards relevant biological pathways.

3.8. Validation of Epic array data using targeted bisulfite sequencing

To assess the reproducibility of the identified differentially methylated CpGs between responders and non-responders, we independently validated the CpG methylation levels at specific sites using an alternative methylation technique, targeted sequencing of bisulfite-converted DNA. Validation was carried out using DNAs from 4 responder and 4 non-responder melanomas to anti-PD1 therapy.

Methylation primers were designed for specific 850K probe locations, including *ERCC1*, *ACSS3*, and *GNA11* (Supplementary Tables 2 and 7) which were the top three genes identified showing the best DNA methylation/gene expression concordance between responders and non-responders. Additionally, primers were designed for the transcription start site (TSS) of *EMP3* as a negative control, as this CpG site was not significantly differentially methylated in the 850K data analysis. Additional loci were not technically validated using this technique due to limited recovery of DNA from the samples.

Targeted methylation sequencing data, which consistently aligned with the results obtained from the Infinium® MethylationEPIC array (single CpG) data across all four loci (refer to the heatmap in Fig. 5A), are shown as both average percentage methylation and as scatterplots showing the percentage methylation at multiple CpGs within the amplimer (Fig. 6). For example, the average methylation levels for multiple CpG sites in *ERCC1*, *ACSS3*, and *GNA11*, as shown in the graphs on the left of Fig. 6, or percentage methylation levels at each CpG site, shown in the graphs on the right of Fig. 6, indicate that there are marked methylation differences between the responder and non-responder melanoma DNAs. Our results from this independent validation technique corresponded very well with the Infinium® MethylationEPIC array alterations in methylation level and the direction of methylation change, technically validating the methylation changes we identified using the Infinium® MethylationEPIC array data.

3.9. Independent validation of DNA methylation differences associated with response to anti-PD1 therapy using an external melanoma cohort

To further corroborate the methylation differences that we observed between melanomas from responding and non-responding patients, we next analysed an external independent Illumina Epic array dataset generated by Ressler and colleagues (GEO: GSE235122) [26]) by using the RnBeads package. Melanoma samples from this dataset were chosen matching as closely as possible our inclusion criteria, and included melanoma samples collected from 24 cutaneous metastatic sites, 28 lymph node metastatic sites, and 9 primary tumours. Samples derived from other different organ sites that were collected from the same treatment-naïve patients were excluded due to possible confounding effects. In total 46 patient samples (18 responders and 28 non-responders, using the authors' classification criteria) were included in the analysis (Supplementary Fig. S3). This analysis revealed significant DNA methylation changes which involved loci that were in common with our data, in thirteen out of thirty-five loci (*TSPEAR-AS1*, *OR51B5*, *PTHLH*, *PRKAA2*, *PAPPA2*, *LINC01606*, *GPRC5A*, *ERC2*, *COL9A2*, *TNFRSF10D*, *ADRB1*, *GRIA4*, *SYT17*), which had been identified above as significant changes in both DNA methylation and gene

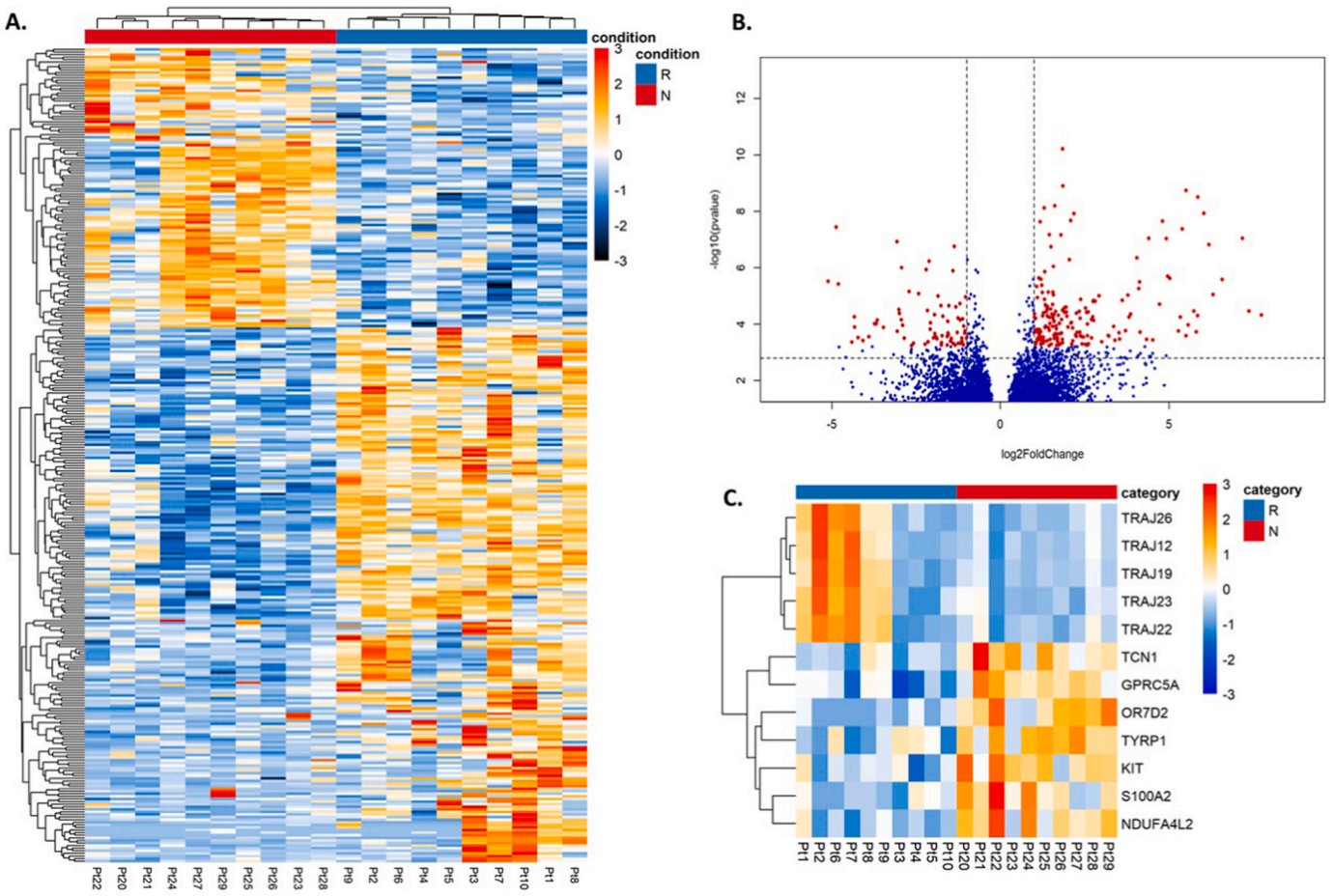

Fig. 4. Differential gene expression analysis between responding and non-responding melanomas. A. Heatmap for the responding and non-responding melanomas showing 315 significantly differentially expressed genes (DEGs). Gene expression values are presented as z-scores. B. A volcano plot representing statistically significant biologically relevant genes with more than 1.5-log2fold change in expression (red dots). C. Responder melanomas exhibited upregulation of immunogenic signature genes, while non-responder melanomas exhibited upregulation of mesenchymal transition associated signature genes. Gene expression values are presented as z-scores.

expression in melanomas from responder versus non-responder patients (Supplementary Table 8). The directions of DNA methylation change, either as hypomethylation or hypermethylation, which were observed in the identified 13 loci, were conserved in the external dataset.

4. Discussion

Immunotherapy resistance, involving complex, as yet unclear mechanisms to avoid immune attack and cell death induced by anti-PD1 therapy, commonly occurs in metastatic melanoma [30]. Epigenetic alterations, including DNA methylation and its subsequent impact on gene expression, may play a significant role in driving resistance to anti-PD1 immunotherapy, while also promoting aggressive phenotypic changes in melanoma cells [36,37]. Moreover, changes in DNA methylation levels have been shown to have a direct involvement in PD-L1 expression levels, further highlighting the role of epigenetic modifications in immune evasion [13].

In this study, we investigated DNA methylation and transcriptomic changes to identify co-ordinated alterations in DNA methylation and gene expression, and their correlation with therapeutic response to anti-PD1 therapy. RNA-seq was employed to explore biologically and functionally relevant processes operating in conjunction with DNA methylation changes in responder versus non-responder melanoma samples. To date, no DNA methylation alterations have been reported in melanoma that are co-ordinately associated with gene expression changes and strongly correlated with response to anti-PD1 ICI therapy.

We applied strict inclusion criteria to identify patients for methylome and transcriptome analysis using archival FFPE melanoma tissues. Our DNA methylation analysis with Illumina Infinium® MethylationEPIC microarrays revealed a set of 2579 significant differentially methylated CpG sites with $\geq$20 % methylation difference between responders and non-responders to anti-PD1 ICI therapy. These CpG sites were distributed across gene bodies, transcriptional start sites (TSS), and 5′ untranslated regions (UTRs), identifying both hypomethylation and hypermethylation changes that correlate with ICI response (Fig. 2).

Integrative analysis of DNA methylation and gene expression changes revealed 35 loci that were significantly altered in both methylation and transcription levels, with consistent up-regulation or down-regulation of genes across all melanoma samples which was correlated with the methylation status. These correlations were statistically significant (p-value $<$0.05, Pearson correlation coefficient $>|0.5|$), (Fig. 5, Supplementary Table 6). In contrast, well-known immune checkpoint mRNAs such as *PD-L1*, *CTLA4*, *TIM3*, *TIGIT*, *LAG3* did not correlate with anti-PD1 response in our melanoma cohort (Supplementary Fig. 2), nor did TMB status [4].

For technical validation of the methylation changes identified in our Epic array data, we employed a targeted bisulfite sequencing approach. This validation focused on several CpGs within selected genes – ERCC1, ACSS3, and GNA11 – which demonstrated significant and reproducible concordance between methylation and gene expression changes. Our results corroborated the differential methylation patterns detected by the Epic array as well as revealing that adjacent CpG sites within these

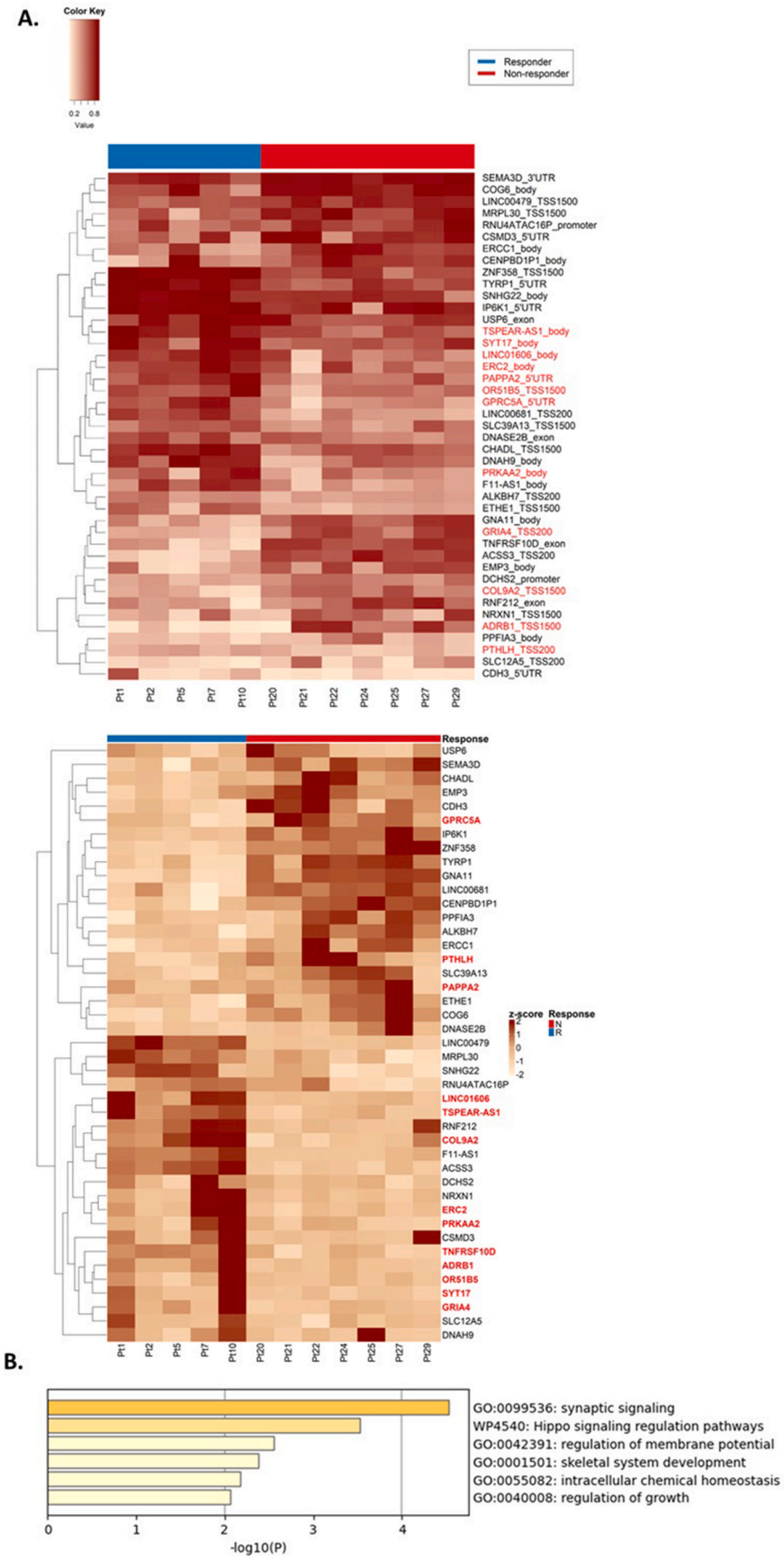

Fig. 5. Concordant DNA methylation and gene expression analysis between responding and non-responding melanomas to anti-PD1 therapy. A. Heatmaps comparing between concordant DNA methylation (top heatmap) and gene expression (bottom heatmap) differences. Methylation values are presented as β values (as described in Fig. 2), and the gene expression values are presented as z-scores. B. Enrichment analysis using differentially methylated/expressed genes.

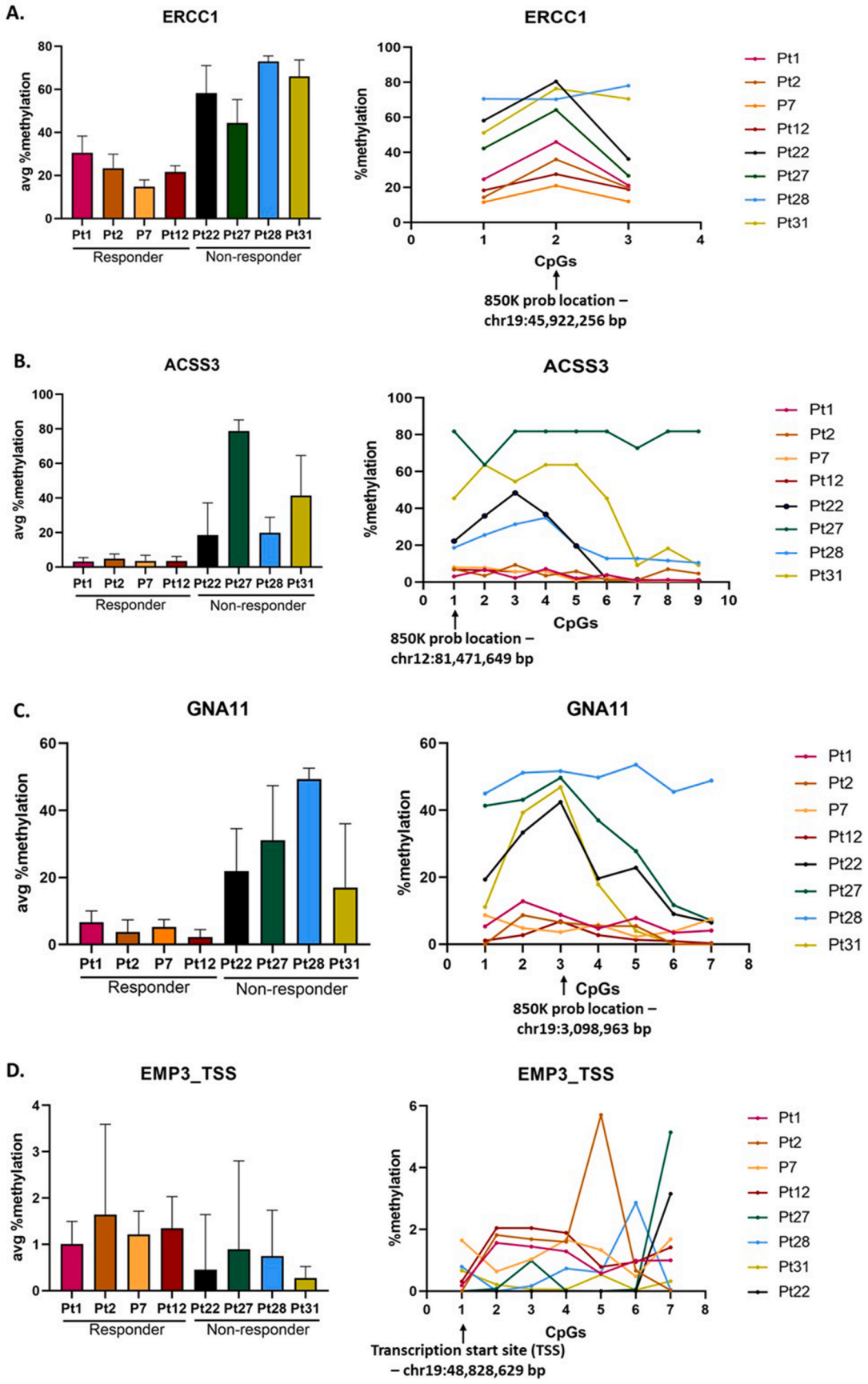

(caption on next page)

Fig. 6. Targeted methylation sequencing in order to validate the 850K methylation data. **A.** ERCC1: 850K probe location was at 45,922,256 bp on chromosome 19q13. **B.** ACSS3: 850K probe location was at 81,471,649 bp on chromosome 12q21. **C.** GNA11: 850K probe location was at 3,098,963 bp on chromosome 19p13. **D.** EMP3: 850K probe location was at 48,828,629 bp on chromosome 19. EMP3 transcription start site (TSS) was designed from 48,828,593 bp – 48,828,794 bp on chromosome 19q13. The bar plots (left side of the figure) represent the average percentage methylation for all CpGs within each specific amplimer for each patient. Alongside the bar graphs are shown scatterplots (right side of the figure), in which dots represent the percentage methylation level (%) of each individual CpG within each amplimer. The amplimers were specifically designed for assessing the immediate region surrounding a single 850K CpG site (arrow) for each melanoma DNA sample. Responder = Pt1, Pt2, Pt7, Pt12. Non-responder = Pt22, Pt27, Pt28, Pt31.

loci also showed similar methylation changes.

Furthermore, we have validated the significant methylation differences observed in thirteen of the thirty-five loci using an independent external dataset (GEO: GSE235122 [26]). These results corroborate our original methylation data, and suggest that 22 of the 35 loci could represent newly identified alterations in melanoma. Among the 22 newly identified loci, promoter hypomethylation in *TYRP1* (*tyrosinase-related protein 1*) has not previously been reported in melanoma, although *TYRP1* overexpression has been associated with melanoma progression and aggressiveness [38].

Of particular note, among the overlapping thirteen loci identified both in our data and in the GEO dataset, missense mutations in *PAPPA2* have previously been shown to stratify beneficiaries of immune checkpoint inhibitors in skin cutaneous melanoma and non-small cell lung cancer patients [39]. In addition, *TNFRSF10D* promoter hypermethylation was found to be strongly associated with relapse-free survival in melanoma patients [40]. Further, *TNFRSF10D* was previously identified as a differentially expressed tumour suppressor gene linked to the survival of melanoma patients [41]. Differential methylation observed at CpGs in *ERCC1*, *ACSS3* and *GNA11* in the independent external dataset was similar to our dataset, though not significantly differentially methylated.

Several differentially expressed genes identified in our RNA-Seq data (Fig. 4C) have previously been associated with poor prognosis, and have been suggested to act as prognostic biomarkers in melanoma. For example, overexpression of *S100A2* [42], *TCN1* [43] and *OR7D2* [44] also induce epithelial-mesenchymal transition (EMT) followed by invasion. In addition, upregulation of T-cell receptor alpha joining genes (*TRAJ26*, *TRAJ23*, *TRAJ19*, *TRAJ12*, *TRAJ22*) was observed in the responder RNA-seq data, consistent with sensitivity to anti-PD1 therapy in responding tumours. Because PD-1 expression on naïve T cells is induced upon T-cell receptor (TCR) activation [45], these data are consistent with a subset of responding tumours containing intrinsically activated T-cells, able to recognize neoantigens presented on tumour cells, through activation of T-cell receptors (TCRs).

Subsequently, we conducted pathway enrichment analysis specifically focusing on hypomethylated CpGs within the TSS region, revealing distinctive biological processes associated with responder and non-responder melanomas. Responding melanomas exhibited enrichment in biological processes such as “Epithelial cell differentiation”, “Stem cell differentiation”, “Regulation of fibroblast growth factor receptor signalling pathway”, and “Regulation of neuron differentiation” (Fig. 3A). Several studies have demonstrated dynamic phenotypic states in melanoma, with the ability to transition between melanocytic and undifferentiated phenotypes [46,47]. Our methylation pathway analyses suggest that responder melanomas may be predominantly enriched with, or have acquired hypomethylated loci indicative of a proliferative phenotype in melanoma cells. These findings align with our previous studies [4], suggesting that responding melanomas are associated with melanocytic gene expression patterns.

Additionally, non-responding melanomas exhibited enrichment of hypomethylated TSS sites associated with processes such as “Formation of the cornified envelope”, “Cell-cell junction assembly”, and “Blood vessel remodelling” (Fig. 3B). Typically, the cornified envelope constitutes a highly insoluble, resilient structure formed during the terminal differentiation of keratinocytes, serving as a protective barrier against environmental factors [48]. Hypomethylation of genes involved in blood vessel remodelling in non-responding melanomas may be associated with trans-differentiation of melanoma cells into endothelial cells, recapitulating embryonic blood vessel development processes [49], which could promote metastasis, tumour progression [50], and the reprogramming of the tumour immune microenvironment [51]. Our findings also align with Chen et al. [52], who proposed a *VEGFA*-related mechanism of therapeutic resistance associated with increased *VEGFA* gene expression in non-responding metastatic melanoma patients treated with PD-1 monoclonal antibodies. Emerging data suggest that ICI resistance could be alleviated by combination therapy with anti-angiogenesis treatment [51,53]. Overall, these observations are consistent with a potential interplay between DNA methylation, cellular phenotype and anti-PD1 therapeutic response in melanoma.

5. Conclusions

We have performed whole genome-scale DNA methylation, and integrated whole transcriptome analysis, carried out using archival FFPE tissues obtained prior to the commencement of anti-PD1 ICI therapy in melanoma patients, to identify potential biomarkers of ICI response. Our study provides new insights into the role of DNA methylation and gene expression changes in anti-PD1 therapy resistance in melanoma, and identifies novel key methylation together with coordinated transcriptional changes, as well as confirming previously identified changes in genes involved in immune evasion and aggressive phenotypic changes. The methylation markers identified here have the potential to predict personalized treatment strategies, and when combined with integrated transcriptional data, may facilitate the identification of a panel of predictive biomarkers of response to anti-PD1 therapy in melanoma.

Ethics approval/patient consent

Ethical approval was granted by the Maria Sklodowska-Curie National Research Institute of Oncology Ethics Committee, Krakow, Poland (KB/430-74/20). All experimental protocols were performed in accordance with the ethical approval, and informed consent was provided by all patients.

CRediT authorship contribution statement

Sultana Mehbuba Hossain: Writing – original draft, Investigation, Formal analysis, Data curation, Conceptualization. **Gregory Gimenez:** Writing – review & editing, Formal analysis, Data curation. **Peter Stockwell:** Writing – review & editing, Software, Formal analysis. **Robert Weeks:** Formal analysis. **Suzan Almomani:** Writing – review & editing. **Gregory T. Jones:** Writing – review & editing, Formal analysis. **Magdalena Ratajska:** Writing – review & editing, Resources. **Mathew Shuen:** Formal analysis. **Basharat Bhat:** Formal analysis. **Janusz Ryś:** Resources. **Bozena Cybulska-Stopa:** Writing – review & editing, Resources. **Agnieszka Harazin-Lechowska:** Writing – review & editing, Resources. **Euan Rodger:** Writing – review & editing. **Christopher Jackson:** Writing – review & editing, Resources, Funding acquisition. **Aniruddha Chatterjee:** Writing – review & editing, Funding acquisition, Conceptualization. **Michael R. Eccles:** Writing – review & editing, Supervision, Project administration, Funding acquisition, Conceptualization.

Data availability

All data have been submitted to the NCBI GEO data repository. The accession number for the transcriptome dataset is GEO: GSE213145. The accession number for the methylome dataset is GEO: GSE264158.

Funding

This work was supported by project grant funding from the Health Research Council of New Zealand, grant number 18/144, grant funding from Otago Medical Research Foundation, and from the Maurice Wilkins Centre for Molecular Biodiscovery, a University of Otago PhD Scholarship (S.M.H.), New Zealand Institute for Cancer Research Trust for Postdoctoral Fellowships (S.M.H. and M.R.) and a Rutherford Discovery Fellowship (A.C.).

Declaration of competing interest

The authors declare that they have no known competing financial interests or personal relationships that could have appeared to influence the work reported in this paper.

Acknowledgements

The authors acknowledge Ryan Powell for his technical advice regarding genomic FFPE DNA restoration.

Appendix A. Supplementary data

Supplementary data to this article can be found online at https://doi.org/10.1016/j.canlet.2025.217638.

References

[1] C. Robert, J. Schachter, G.V. Long, A. Arance, J.J. Grob, L. Mortier, A. Daud, M. S. Carlino, C. McNeil, M. Lotem, et al., Pembrolizumab versus ipilimumab in advanced melanoma, N. Engl. J. Med. 372 (2015) 2521–2532, https://doi.org/10.1056/NEJMoa1503093.

[2] H. Li, P.A. van der Merwe, S. Sivakumar, Biomarkers of response to PD-1 pathway blockade, Br. J. Cancer 126 (2022) 1663–1675, https://doi.org/10.1038/s41416-022-01743-4.

[3] S.M. Hossain, C.F. Lynch-Sutherland, A. Chatterjee, E.C. Macaulay, M.R. Eccles, Can immune suppression and epigenome regulation in placenta offer novel insights into cancer immune evasion and immunotherapy resistance? Epigenomes 5 (2021) https://doi.org/10.3390/epigenomes5030016.

[4] S.M. Hossain, G. Gimenez, P.A. Stockwell, P. Tsai, C.G. Print, J. Rys, B. Cybulska-Stopa, M. Ratajska, A. Harazin-Lechowska, S. Almomani, et al., Innate immune checkpoint inhibitor resistance is associated with melanoma sub-types exhibiting invasive and de-differentiated gene expression signatures, Front. Immunol. 13 (2022), https://doi.org/10.3389/fimmu.2022.955063.

[5] S.M. Hossain, M.R. Eccles, Phenotype switching and the melanoma microenvironment; impact on immunotherapy and drug resistance, Int. J. Mol. Sci. 24 (2023), https://doi.org/10.3390/ijms24021601.

[6] B. El Osta, F. Hu, R. Sadek, R. Chintalapally, S.C. Tang, Not all immune-checkpoint inhibitors are created equal: meta-analysis and systematic review of immune-related adverse events in cancer trials, Crit. Rev. Oncol.-Hematol. 119 (2017) 1–12, https://doi.org/10.1016/j.critrevonc.2017.09.002.

[7] C. Robert, A. Ribas, J.D. Wolchok, F.S. Hodi, O. Hamid, R. Kefford, J.S. Weber, A. M. Joshua, W.J. Hwu, T.C. Gangadhar, et al., Anti-programmed-death-receptor-1 treatment with pembrolizumab in ipilimumab-refractory advanced melanoma: a randomised dose-comparison cohort of a phase 1 trial, Lancet (London, England) 384 (2014) 1109–1117, https://doi.org/10.1016/s0140-6736(14)60958-2.

[8] D. Schadendorf, F.S. Hodi, C. Robert, J.S. Weber, K. Margolin, O. Hamid, D. Patt, T. T. Chen, D.M. Berman, J.D. Wolchok, Pooled analysis of long-term survival data from phase II and phase III trials of ipilimumab in unresectable or metastatic melanoma, J. Clin. Oncol. : Off. J. Am. Soc. Clin. Oncol. 33 (2015) 1889–1894, https://doi.org/10.1200/jco.2014.56.2736.

[9] S.M. Hossain, C. Carpenter, M.R. Eccles, Genomic and epigenomic biomarkers of immune checkpoint immunotherapy response in melanoma: current and future perspectives, Int. J. Mol. Sci. 25 (2024), https://doi.org/10.3390/ijms25137252.

[10] E.C. Paver, W.A. Cooper, A.J. Colebatch, P.M. Ferguson, S.K. Hill, T. Lum, J.S. Shin, S. O'Toole, L. Anderson, R.A. Scolyer, et al., Programmed death ligand-1 (PD-L1) as a predictive marker for immunotherapy in solid tumours: a guide to immunohistochemistry implementation and interpretation, Pathology 53 (2021) 141–156, https://doi.org/10.1016/j.pathol.2020.10.007.

[11] V. Audrito, S. Serra, A. Stingi, F. Orso, F. Gaudino, C. Bologna, F. Neri, G. Garaffo, R. Nassini, G. Baroni, et al., PD-L1 up-regulation in melanoma increases disease aggressiveness and is mediated through miR-17-5p, Oncotarget 8 (2017) 15894–15911, https://doi.org/10.18632/oncotarget.15213.

[12] M.J. Smyth, S.F. Ngiow, A. Ribas, M.W. Teng, Combination cancer immunotherapies tailored to the tumour microenvironment, Nat. Rev. Clin. Oncol. 13 (2016) 143–158, https://doi.org/10.1038/nrclinonc.2015.209.

[13] A. Chatterjee, E.J. Rodger, A. Ahn, P.A. Stockwell, M. Parry, J. Motwani, S. J. Gallagher, E. Shklovskaya, J. Tiffen, M.R. Eccles, et al., Marked global DNA hypomethylation is associated with constitutive PD-L1 expression in melanoma, iScience 4 (2018) 312–325, https://doi.org/10.1016/j.isci.2018.05.021.

[14] G. Yu, Y. Wu, W. Wang, J. Xu, X. Lv, X. Cao, T. Wan, Low-dose decitabine enhances the effect of PD-1 blockade in colorectal cancer with microsatellite stability by re-modulating the tumor microenvironment, Cell. Mol. Immunol. 16 (2019) 401–409, https://doi.org/10.1038/s41423-018-0026-y.

[15] K.K. Wong, R. Hassan, N.S. Yaacob, Hypomethylating agents and immunotherapy: therapeutic synergism in acute myeloid leukemia and myelodysplastic syndromes, Front. Oncol. 11 (2021) 624742, https://doi.org/10.3389/fonc.2021.624742.

[16] Y. Assenov, F. Müller, P. Lutsik, J. Walter, T. Lengauer, C. Bock, Comprehensive analysis of DNA methylation data with RnBeads, Nat. Methods 11 (2014) 1138–1140, https://doi.org/10.1038/nmeth.3115.

[17] F. Müller, M. Scherer, Y. Assenov, P. Lutsik, J. Walter, T. Lengauer, C. Bock, RnBeads 2.0: comprehensive analysis of DNA methylation data, Genome Biol. 20 (2019) 55, https://doi.org/10.1186/s13059-019-1664-9.

[18] A. Chatterjee, A. Ahn, E.J. Rodger, P.A. Stockwell, M.R. Eccles, A guide for designing and analyzing RNA-seq data, Methods Mol. Biol. 1783 (2018) 35–80, https://doi.org/10.1007/978-1-4939-7834-2_3.

[19] M. Pertea, D. Kim, G.M. Pertea, J.T. Leek, S.L. Salzberg, Transcript-level expression analysis of RNA-seq experiments with HISAT, StringTie and Ballgown, Nat. Protoc. 11 (2016) 1650–1667, https://doi.org/10.1038/nprot.2016.095.

[20] Y. Liao, G.K. Smyth, W. Shi, featureCounts: an efficient general purpose program for assigning sequence reads to genomic features, Bioinformatics 30 (2014) 923–930, https://doi.org/10.1093/bioinformatics/btt656.

[21] M.A. Van De Wiel, G.G. Leday, L. Pardo, H. Rue, A.W. Van Der Vaart, W.N. Van Wieringen, Bayesian analysis of RNA sequencing data by estimating multiple shrinkage priors, Biostatistics 14 (2013) 113–128, https://doi.org/10.1093/biostatistics/kxs031.

[22] M.I. Love, W. Huber, S. Anders, Moderated estimation of fold change and dispersion for RNA-seq data with DESeq2, Genome Biol. 15 (2014) 550, https://doi.org/10.1186/s13059-014-0550-8.

[23] L.C. Li, R. Dahiya, MethPrimer: designing primers for methylation PCRs, Bioinformatics 18 (2002) 1427–1431, https://doi.org/10.1093/bioinformatics/18.11.1427.

[24] J. Zhang, K. Kobert, T. Flouri, A. Stamatakis, PEAR: a fast and accurate Illumina Paired-End reAd mergeR, Bioinformatics 30 (2014) 614–620, https://doi.org/10.1093/bioinformatics/btt593.

[25] C. Bock, S. Reither, T. Mikeska, M. Paulsen, J. Walter, T. Lengauer, BiQ Analyzer: visualization and quality control for DNA methylation data from bisulfite sequencing, Bioinformatics 21 (2005) 4067–4068, https://doi.org/10.1093/bioinformatics/bti652.

[26] J.M. Ressler, E. Tomasich, T. Hatziioannou, H. Ringl, G. Heller, R. Silmbrod, L. Gottmann, A.M. Starzer, N. Zila, P. Tschandl, et al., DNA methylation signatures correlate with response to immune checkpoint inhibitors in metastatic melanoma, Targeted Oncol. 19 (2024) 263–275, https://doi.org/10.1007/s11523-024-01041-4.

[27] K. Filipski, M. Scherer, K.N. Zeiner, A. Bucher, J. Kleemann, P. Jurmeister, T. I. Hartung, M. Meissner, K.H. Plate, T.R. Fenton, et al., DNA methylation-based prediction of response to immune checkpoint inhibition in metastatic melanoma, J. Immunother. Cancer 9 (2021), https://doi.org/10.1136/jitc-2020-002226.

[28] W. Hugo, J.M. Zaretsky, L. Sun, C. Song, B.H. Moreno, S. Hu-Lieskovan, B. Berent-Maoz, J. Pang, B. Chmielowski, G. Cherry, et al., Genomic and transcriptomic features of response to anti-PD-1 therapy in metastatic melanoma, Cell 168 (2017) 542, https://doi.org/10.1016/j.cell.2017.01.010.

[29] F. Newell, I. Pires da Silva, P.A. Johansson, A.M. Menzies, J.S. Wilmott, V. Addala, M.S. Carlino, H. Rizos, K. Nones, J.J. Edwards, et al., Multiomic profiling of checkpoint inhibitor-treated melanoma: identifying predictors of response and resistance, and markers of biological discordance, Cancer Cell 40 (2022) 88–102. e107, https://doi.org/10.1016/j.ccell.2021.11.012.

[30] N. Riaz, J.J. Havel, V. Makarov, A. Desrichard, W.J. Urba, J.S. Sims, F.S. Hodi, S. Martín-Algarra, R. Mandal, W.H. Sharfman, et al., Tumor and microenvironment evolution during immunotherapy with nivolumab, Cell 171 (2017) 934–949.e916, https://doi.org/10.1016/j.cell.2017.09.028.

[31] T.N. Gide, C. Quek, A.M. Menzies, A.T. Tasker, P. Shang, J. Holst, J. Madore, S. Y. Lim, R. Velickovic, M. Wongchenko, et al., Distinct immune cell populations define response to anti-PD-1 monotherapy and anti-PD-1/anti-CTLA-4 combined therapy, Cancer Cell 35 (2019) 238–255.e236, https://doi.org/10.1016/j.ccell.2019.01.003.

[32] R.J. Lu, P.Y. Lin, M.R. Yen, B.H. Wu, P.Y. Chen, MethylC-analyzer: a comprehensive downstream pipeline for the analysis of genome-wide DNA methylation, Bot. Stud. 64 (2023) 1, https://doi.org/10.1186/s40529-022-00366-5.

[33] G. Ferrara, G. Argenziano, The WHO 2018 classification of cutaneous melanocytic neoplasms: suggestions from routine practice, Front. Oncol. 11 (2021) 675296, https://doi.org/10.3389/fonc.2021.675296.

[34] A.M. Goodman, S. Kato, L. Bazhenova, S.P. Patel, G.M. Frampton, V. Miller, P. J. Stephens, G.A. Daniels, R. Kurzrock, Tumor mutational burden as an

independent predictor of response to immunotherapy in diverse cancers, Mol. Cancer Therapeut. 16 (2017) 2598–2608, https://doi.org/10.1158/1535-7163.Mct-17-0386.
[35] Y. Zhou, B. Zhou, L. Pache, M. Chang, A.H. Khodabakhshi, O. Tanaseichuk, C. Benner, S.K. Chanda, Metascape provides a biologist-oriented resource for the analysis of systems-level datasets, Nat. Commun. 10 (2019) 1523, https://doi.org/10.1038/s41467-019-09234-6.
[36] L. Villanueva, D. Álvarez-Errico, M. Esteller, The contribution of epigenetics to cancer immunotherapy, Trends Immunol. 41 (2020) 676–691, https://doi.org/10.1016/j.it.2020.06.002.
[37] S. Romero-Garcia, H. Prado-Garcia, A. Carlos-Reyes, Role of DNA methylation in the resistance to therapy in solid tumors, Front. Oncol. 10 (2020) 1152, https://doi.org/10.3389/fonc.2020.01152.
[38] P. El Hajj, D. Gilot, M. Migault, A. Theunis, L.C. van Kempen, F. Salés, H. Fayyad-Kazan, B. Badran, D. Larsimont, A. Awada, et al., SNPs at miR-155 binding sites of TYRP1 explain discrepancy between mRNA and protein and refine TYRP1 prognostic value in melanoma, Br. J. Cancer 113 (2015) 91–98, https://doi.org/10.1038/bjc.2015.194.
[39] Y. Dong, L. Zhao, J. Duan, H. Bai, D. Chen, S. Li, Y. Yu, M. Xiao, Q. Zhang, Q. Duan, et al., PAPPA2 mutation as a novel indicator stratifying beneficiaries of immune checkpoint inhibitors in skin cutaneous melanoma and non-small cell lung cancer, Cell Prolif. 55 (2022) e13283, https://doi.org/10.1111/cpr.13283.
[40] V.F. Bonazzi, D.J. Nancarrow, M.S. Stark, R.J. Moser, G.M. Boyle, L.G. Aoude, C. Schmidt, N.K. Hayward, Cross-platform array screening identifies COL1A2, THBS1, TNFRSF10D and UCHL1 as genes frequently silenced by methylation in melanoma, PLoS One 6 (2011) e26121, https://doi.org/10.1371/journal.pone.0026121.
[41] G. Ratzinger, S. Mitteregger, B. Wolf, R. Berger, B. Zelger, G. Weinlich, P. Fritsch, G. Goebel, H. Fiegl, Association of TNFRSF10D DNA-methylation with the survival of melanoma patients, Int. J. Mol. Sci. 15 (2014) 11984–11995, https://doi.org/10.3390/ijms150711984.
[42] S. Naz, M. Bashir, P. Ranganathan, P. Bodapati, V. Santosh, P. Kondaiah, Protumorigenic actions of S100A2 involve regulation of PI3/Akt signaling and functional interaction with Smad3, Carcinogenesis 35 (2014) 14–23, https://doi.org/10.1093/carcin/bgt287.
[43] G.J. Liu, Y.J. Wang, M. Yue, L.M. Zhao, Y.D. Guo, Y.P. Liu, H.C. Yang, F. Liu, X. Zhang, L.H. Zhi, et al., High expression of TCN1 is a negative prognostic biomarker and can predict neoadjuvant chemosensitivity of colon cancer, Sci. Rep. 10 (2020) 11951, https://doi.org/10.1038/s41598-020-68150-8.
[44] G. Sanz, I. Leray, A. Dewaele, J. Sobilo, S. Lerondel, S. Bouet, D. Grébert, R. Monnerie, E. Pajot-Augy, L.M. Mir, Promotion of cancer cell invasiveness and metastasis emergence caused by olfactory receptor stimulation, PLoS One 9 (2014) e85110, https://doi.org/10.1371/journal.pone.0085110.
[45] S. Chikuma, S. Terawaki, T. Hayashi, R. Nabeshima, T. Yoshida, S. Shibayama, T. Okazaki, T. Honjo, PD-1-mediated suppression of IL-2 production induces CD8+ T cell anergy *in vivo*, J. Immunol. (182) (2009) 6682–6689, https://doi.org/10.4049/jimmunol.0900080. Baltimore, Md. : 1950.
[46] K.S. Hoek, O.M. Eichhoff, N.C. Schlegel, U. Döbbeling, N. Kobert, L. Schaerer, S. Hemmi, R. Dummer, *In vivo* switching of human melanoma cells between proliferative and invasive states, Cancer Res. 68 (2008) 650–656, https://doi.org/10.1158/0008-5472.Can-07-2491.
[47] K.S. Hoek, C.R. Goding, Cancer stem cells versus phenotype-switching in melanoma, Pigment Cell Melanoma Res. 23 (2010) 746–759, https://doi.org/10.1111/j.1755-148X.2010.00757.x.
[48] A. Ishida-Yamamoto, H. Iizuka, Structural organization of cornified cell envelopes and alterations in inherited skin disorders, Exp. Dermatol. 7 (1998) 1–10, https://doi.org/10.1111/j.1600-0625.1998.tb00295.x.
[49] D.M. Noden, Embryonic origins and assembly of blood vessels, Am. Rev. Respir. Dis. 140 (1989) 1097–1103, https://doi.org/10.1164/ajrccm/140.4.1097.
[50] P. Carmeliet, R.K. Jain, Molecular mechanisms and clinical applications of angiogenesis, Nature 473 (2011) 298–307, https://doi.org/10.1038/nature10144.
[51] M. Yi, D. Jiao, S. Qin, Q. Chu, K. Wu, A. Li, Synergistic effect of immune checkpoint blockade and anti-angiogenesis in cancer treatment, Mol. Cancer 18 (2019) 60, https://doi.org/10.1186/s12943-019-0974-6.
[52] P.L. Chen, W. Roh, A. Reuben, Z.A. Cooper, C.N. Spencer, P.A. Prieto, J.P. Miller, R. L. Bassett, V. Gopalakrishnan, K. Wani, et al., Analysis of immune signatures in longitudinal tumor samples yields insight into biomarkers of response and mechanisms of resistance to immune checkpoint blockade, Cancer Discov. 6 (2016) 827–837, https://doi.org/10.1158/2159-8290.Cd-15-1545.
[53] Q. Wang, J. Gao, W. Di, X. Wu, Anti-angiogenesis therapy overcomes the innate resistance to PD-1/PD-L1 blockade in VEGFA-overexpressed mouse tumor models, Cancer Immunol. Immunother. : CII 69 (2020) 1781–1799, https://doi.org/10.1007/s00262-020-02576-x.